

Unconventional Bloch-Grüneisen Scattering in Hybrid Bose-Fermi Systems

K. H. A. Villegas,¹ Meng Sun,^{1,2} V. M. Kovalev,^{3,4} and I. G. Savenko^{1,2,3}

¹Center for Theoretical Physics of Complex Systems, Institute for Basic Science (IBS), Daejeon 34126, Korea

²Basic Science Program, Korea University of Science and Technology (UST), Daejeon 34113, Korea

³A. V. Rzhanov Institute of Semiconductor Physics, Siberian Branch of Russian Academy of Sciences, Novosibirsk 630090, Russia

⁴Department of Applied and Theoretical Physics, Novosibirsk State Technical University, Novosibirsk 630073, Russia



(Received 30 January 2019; revised manuscript received 25 March 2019; published 27 August 2019)

We report on the novel mechanism of electron scattering in hybrid Bose-Fermi systems consisting of a two-dimensional electron gas in the vicinity of an exciton condensate: We show that in certain ranges of temperatures, the bogolon-pair-mediated scattering proves to be dominating over the conventional acoustic phonon channel, over the single-bogolon scattering, and over the scattering on impurities. We develop a microscopic theory of this effect, focusing on GaAs and MoS₂ materials, and we find the principal temperature dependence of resistivity, distinct from the conventional phonon-mediated processes. Further, we scrutinize parameters and suggest a way to design composite samples with predefined electron mobilities, and we propose a mechanism of electron pairing for superconductivity.

DOI: 10.1103/PhysRevLett.123.095301

Hybrid Bose-Fermi systems essentially represent a layer of fermions, usually two-dimensional electron gas (2DEG), coupled to another layer of bosons, such as excitons, exciton polaritons, or Cooper pairs. The interplay between Bose and Fermi particles leads to various novel fascinating phenomena, interesting from both the technological and fundamental physics perspectives. For instance, in a hybrid two-dimensional electron gas–superconductor system, it became possible to realize the long-sought Majorana fermion [1–4]. There were also proposed new mechanisms of electron pairing [5] in a hybrid setup involving exciton polaritons in a semiconductor microcavity, opening a possibility for optically controlled superconductivity [6]. Furthermore, the interplay between the polaritons and phonons can enhance the critical temperature of the superconductor [7]. These results pave the way for the realization of a high-temperature conventional Bardeen-Cooper-Schrieffer (BCS) superconductivity.

In solid-state systems, bosons can undergo a phase transition to a Bose-Einstein condensate (BEC), which has been reported in GaAs [8] and predicted in MoS₂ materials [9]. In a hybrid system containing a BEC, there can appear magnetically controlled lasing, the Mott phase transition from an ordered state to electron-hole plasma [10], giant Fano resonances [11], which are also shown to occur for superconductor hybrids [12], and supersolidity [13]. Returning to the fermionic subsystem, studies of the electron transport in 2DEG have many technological applications, especially in the context of interface physics [14–16], where 2DEG exhibits rich phenomena such as the anomalous magnetoresistance and the Hall effect [17–19], two-dimensional metallic conductivity [20,21], superconductivity, and ferromagnetism [22–25]. Electron scattering on acoustic phonons and disorder plays a major role in all these phenomena [26–38].

However, the emerging topic of combining a 2DEG with a BEC demands the study of the electron transport in hybrid systems and forces us to confront new types of interactions beyond the conventional phonon and impurity channels [39–42]. In this Letter, we reexamine the electron transport in hybrid systems and report on the unconventional mechanism of the electron scattering which is due to the interaction with the Bogoliubov excitations or bogolons [43,44]. The bogolons represent excitations over the BEC and, similar to acoustic phonons, have a linear spectrum at small momenta. While one may naively argue that the bogolon scattering should be similar to the phonon-assisted case, with the acoustic phonon sound velocity simply replaced by the bogolon sound velocity, we will show that this is not at all the case, and the difference turns out to be fundamental.

Let us consider the system presented in Fig. 1, consisting of a 2DEG with a parabolic dispersion of electrons and a

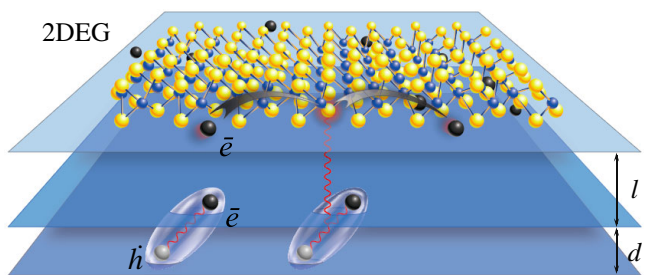


FIG. 1. System schematic. Bogolon-mediated electron scattering in 2DEG in a GaAs layer, located at the distance l from a two-dimensional dipolar exciton gas, residing in two parallel layers (of GaAs or MoS₂), which are at the distance d from each other. The particles are coupled via the Coulomb interaction.

layer of the Bose-condensed exciton gas [43–45]. The two layers are spatially separated and coupled by the Coulomb interaction [11,13], described by the Hamiltonian

$$V = \int d\mathbf{r} \int d\mathbf{R} \Psi_{\mathbf{r}}^{\dagger} \Psi_{\mathbf{r}} g(\mathbf{r} - \mathbf{R}) \Phi_{\mathbf{R}}^{\dagger} \Phi_{\mathbf{R}}, \quad (1)$$

where $\Psi_{\mathbf{r}}$ and $\Phi_{\mathbf{R}}$ are the field operators of electrons and excitons, respectively; $g(\mathbf{r} - \mathbf{R})$ is the Coulomb interaction term; \mathbf{r} is the coordinate in the 2DEG plane; and \mathbf{R} is the exciton center-of-mass coordinate.

Since the excitons are in the BEC phase, we will use the model of weakly interacting Bose gas. Then $\Phi_{\mathbf{R}} = \sqrt{n_c} + \varphi_{\mathbf{R}}$, where n_c is the density of particles in the condensate and $\varphi_{\mathbf{R}}$ is the field operator for the bogolons. Then Eq. (1) splits into two terms:

$$\begin{aligned} V_1 &= \sqrt{n_c} \int d\mathbf{r} \Psi_{\mathbf{r}}^{\dagger} \Psi_{\mathbf{r}} \int d\mathbf{R} g(\mathbf{r} - \mathbf{R}) [\varphi_{\mathbf{R}}^{\dagger} + \varphi_{\mathbf{R}}], \\ V_2 &= \int d\mathbf{r} \Psi_{\mathbf{r}}^{\dagger} \Psi_{\mathbf{r}} \int d\mathbf{R} g(\mathbf{r} - \mathbf{R}) \varphi_{\mathbf{R}}^{\dagger} \varphi_{\mathbf{R}}. \end{aligned} \quad (2)$$

Furthermore, we express the field operators as the Fourier series

$$\begin{aligned} \varphi_{\mathbf{R}}^{\dagger} + \varphi_{\mathbf{R}} &= \frac{1}{L} \sum_{\mathbf{p}} e^{i\mathbf{p}\cdot\mathbf{R}} [(u_{\mathbf{p}} + v_{-\mathbf{p}}) b_{\mathbf{p}} + (v_{\mathbf{p}} + u_{-\mathbf{p}}) b_{-\mathbf{p}}^{\dagger}], \\ \Psi_{\mathbf{r}} &= \frac{1}{L} \sum_{\mathbf{k}} e^{i\mathbf{k}\cdot\mathbf{r}} c_{\mathbf{k}}, \quad \text{and} \quad \Psi_{\mathbf{r}}^{\dagger} = \frac{1}{L} \sum_{\mathbf{k}} e^{-i\mathbf{k}\cdot\mathbf{r}} c_{\mathbf{k}}^{\dagger}, \end{aligned} \quad (3)$$

where $b_{\mathbf{p}}$ ($c_{\mathbf{k}}$) and $b_{\mathbf{p}}^{\dagger}$ ($c_{\mathbf{k}}^{\dagger}$) are the bogolon (electron) annihilation and creation operators, respectively, and L is the length of the structure. The Bogoliubov coefficients read [46]

$$\begin{aligned} u_{\mathbf{p}}^2 &= 1 + v_{\mathbf{p}}^2 = \frac{1}{2} \left(1 + \left[1 + \frac{(Ms^2)^2}{\omega_{\mathbf{p}}^2} \right]^{1/2} \right), \\ u_{\mathbf{p}} v_{\mathbf{p}} &= -\frac{Ms^2}{2\omega_{\mathbf{p}}}, \end{aligned} \quad (4)$$

where M is the exciton mass, $s = \sqrt{\kappa n_c / M}$ is the sound velocity, $\kappa = e_0^2 d / \epsilon$ is the exciton-exciton interaction strength in the reciprocal space, e_0 is electron charge, ϵ is the dielectric function, $\omega_{\mathbf{k}} = sk(1 + k^2 \xi^2)^{1/2}$ is the spectrum of bogolons, and $\xi = \hbar / (2Ms)$ is the healing length. Combining Eqs. (2) and (3), we find

$$\begin{aligned} V_1 &= \frac{\sqrt{n_c}}{L} \sum_{\mathbf{k}, \mathbf{p}} g_{\mathbf{p}} [(v_{\mathbf{p}} + u_{-\mathbf{p}}) b_{-\mathbf{p}}^{\dagger} \\ &\quad + (u_{\mathbf{p}} + v_{-\mathbf{p}}) b_{\mathbf{p}}] c_{\mathbf{k}+\mathbf{p}}^{\dagger} c_{\mathbf{k}}, \end{aligned} \quad (5)$$

$$\begin{aligned} V_2 &= \frac{1}{L^2} \sum_{\mathbf{k}, \mathbf{p}, \mathbf{q}} g_{\mathbf{p}} (u_{\mathbf{q}-\mathbf{p}} u_{\mathbf{q}} b_{\mathbf{q}-\mathbf{p}}^{\dagger} b_{\mathbf{q}} + u_{\mathbf{q}-\mathbf{p}} v_{\mathbf{q}} b_{\mathbf{q}-\mathbf{p}}^{\dagger} b_{-\mathbf{q}}^{\dagger} \\ &\quad + v_{\mathbf{q}-\mathbf{p}} u_{\mathbf{q}} b_{-\mathbf{q}+\mathbf{p}} b_{\mathbf{q}} + v_{\mathbf{q}-\mathbf{p}} v_{\mathbf{q}} b_{-\mathbf{q}+\mathbf{p}} b_{-\mathbf{q}}^{\dagger}) c_{\mathbf{k}+\mathbf{p}}^{\dagger} c_{\mathbf{k}}, \end{aligned} \quad (6)$$

where $g_{\mathbf{p}} = e_0^2 (1 - e^{-pd}) e^{-pl} / (2\epsilon p)$ is the Fourier image of the electron-exciton interaction. Equations (5) and (6) give matrix elements of electron scattering in two conceptually different processes within the same (first) order with respect to the interaction strength $g_{\mathbf{p}}$. The contribution V_1 is responsible for the electron scattering with the emission or absorption of a single Bogoliubov quantum (which we will call *1b* processes), whereas V_2 describes the electron scattering mediated by the emission or absorption of a pair of bogolons (which we will refer to as *2b* processes).

To investigate the principal T dependence of 1b-mediated resistivity at low temperatures, we will adopt the Bloch-Grüneisen formalism [47,48], which was originally used to describe electron-phonon interaction. We start from the Boltzmann equation

$$e_0 \mathbf{E} \cdot \frac{\partial f}{\hbar \partial \mathbf{p}} = I\{f\}, \quad (7)$$

where f is the electron distribution function, \mathbf{p} is the wave vector, \mathbf{E} is an external electric field, and $I\{f\}$ is the collision integral involving 1b scattering processes, as shown in Figs. 2(a) and 2(b) (see Appendix A in the Supplemental Material [49] for the explicit form of I and other details of derivation). For not-too-strong electric fields, f can be expanded as

$$f = f^0(\epsilon_p) - \left(-\frac{\partial f^0}{\partial \epsilon_p} \right) \phi_{\mathbf{p}}, \quad (8)$$

where $p \equiv |\mathbf{p}|$, $f^0(\epsilon_p)$ is the Fermi-Dirac distribution. The function $\phi_{\mathbf{p}}$ is the change in energy of the electron due to the applied field. Without the loss of generality, we define this electric field to be directed along the x axis and use the ansatz

$$\phi_{\mathbf{p}} = (e_0 E_x) (\hbar m^{-1} p_x) \tau(\epsilon_p), \quad (9)$$

where m is the effective electron mass in the 2DEG and $\tau(\epsilon_p)$ is the relaxation time. This ansatz finds its explanation in Fig. 2(g): The factor $e_0 E_x$ is the force acting on the electron, while $\hbar m^{-1} p_x$ is the electron velocity. The function $\phi_{\mathbf{p}}$ therefore gives the work done by the electric field on the electron during the time $\tau(\epsilon_p)$.

Using Eqs. (7)–(9), we find the average value of scattering time [49] and then the 1b-mediated resistivity, which is the first crucial formula in this Letter:

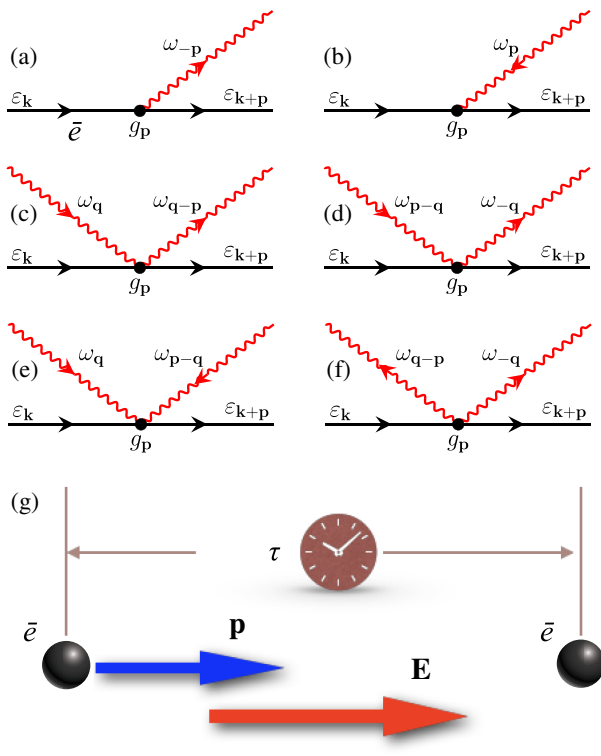


FIG. 2. Feynman diagrams for the scattering processes: straight black lines represent the electrons, while the wiggly red lines represent the bogolons. (a),(b) Single-bogolon scattering events. (c)–(f) Two-bogolon scattering. (g) Schematic of the electron distribution function [ansatz (9)] in the Boltzmann equation: the work done by the electric field \mathbf{E} on the electron with wave vector \mathbf{p} during the relaxation time τ changes the electron energy.

$$\rho^{(1)} = \frac{\pi\hbar^3\xi_I^2}{e_0^2ME_F} \sum_{n=0}^{\infty} \frac{(-2)^n l^n \gamma_n}{n!(\hbar s)^{n+4}} (k_B T)^{n+4}, \quad (10)$$

where $\xi_I = e_0^2 d \sqrt{n_c}/2e$, E_F is the Fermi energy, $\gamma_n = (n+3)! \zeta(n+3)/[(2\pi)^2 k_B T_{BG}]$, $T_{BG} = 2\hbar s k_F/k_B$ is the Bloch-Grüneisen temperature with k_F the Fermi wave vector, k_B is the Boltzmann constant, and $\zeta(x)$ is the Riemann zeta function. The leading term in Eq. (10) if $T \ll T_{BG}$ reads

$$\rho^{(1)} \approx \frac{\pi\hbar^3\xi_I^2}{e_0^2ME_F} \frac{3!\zeta(3)}{(2\pi)^2 k_B T_{BG}} \left(\frac{k_B T}{\hbar s}\right)^4, \quad (11)$$

hence the 1b resistivity behaves as $\rho^{(1)} \propto T^4$ at low temperatures.

The 2b resistivity can also be derived from Eq. (7). The collision integral now expresses the net scattering into a state with momentum $\hbar\mathbf{p}$, involving a pair of bogolons, as shown in Figs. 2(c)–2(f) (see also Appendix B in Ref. [49]). After some unwieldy derivations, we find

$$\rho^{(2)} = \frac{s^2}{8\pi^2 e_0^2 m v_F^5} \int_{L^{-1}}^{\infty} \frac{k^2 g_k^2 dk}{\sinh^2[\frac{\hbar s k}{2k_B T}]} \ln(kL), \quad (12)$$

where v_F is the Fermi velocity. This formula is the central result of this Letter. To find Eq. (12), we used the approximation $v_F \gg s$ and introduced the infrared cutoff L^{-1} for the wave-vector integrals, necessary for the convergence. The physical meaning of this cutoff is the absence of fluctuations with wavelength larger than L . This cutoff can also be related to the critical temperature of the Bose-Einstein condensation in a finite trap of length L [50]. Indeed, a BEC cannot form in infinite homogeneous 2D systems at finite temperatures [51]; thus, a trapping with the characteristic size L is required [43].

We can further extract the temperature dependences for the two limits [49]. At low temperatures $T \ll T_{BG}$,

$$\rho^{(2)} \approx \frac{s^2 e_0^2 d^2}{2v_F^5 \epsilon^2} \left(\frac{T}{T_{BG}}\right)^3 \frac{\pi}{6(2l)^3} \ln\left(\frac{L}{2l}\right), \quad (13)$$

while at high temperatures $T \gg T_{BG}$,

$$\rho^{(2)} \approx \frac{s^2 e_0^2 d^2}{2v_F^5 \epsilon^2} \left(\frac{T}{T_{BG}}\right)^2 \frac{1}{(2l)^3} \ln\left(\frac{L}{2l}\right). \quad (14)$$

Comparing with Eq. (11), we conclude that 2b processes should dominate over 1b processes at very low temperatures. However, in this range the scattering on impurities is usually the strongest, hindering the possibility to observe low-temperature asymptotics. Figure 3 shows the temperature behavior of different principal contributions to resistivity. In order to compare the bogolon-mediated scattering with the scattering on phonons and impurities, we use the theoretical and experimental results reported elsewhere [52–57] and the parameters characteristic of a 2DEG in GaAs and excitons in both the GaAs and MoS₂ materials [58].

Figure 3 shows the resistivity dependence on temperature in the range 1–50 K. We use the concentration of impurities $n_i = 10^9 \text{ cm}^{-2}$, which is attainable in high-quality GaAs 2DEG [62,63]. The yellow shaded region highlights the low-temperature regime $T \ll T_{BG}$, where for both the GaAs and MoS₂, $T_{BG} \approx 80$ K. In this regime, the impurity scattering dominates even in high-quality GaAs 2DEG. However, if $T > 14$ K, we see that the 2b scattering contribution to the resistivity can become an order of magnitude larger than all other contributions if the double quantum well is based on MoS₂ material. The impurity, phonon, and single-Bogoliubov quantum have comparable contributions in the temperature range 20–50 K. The critical temperature of exciton quasicondensa-

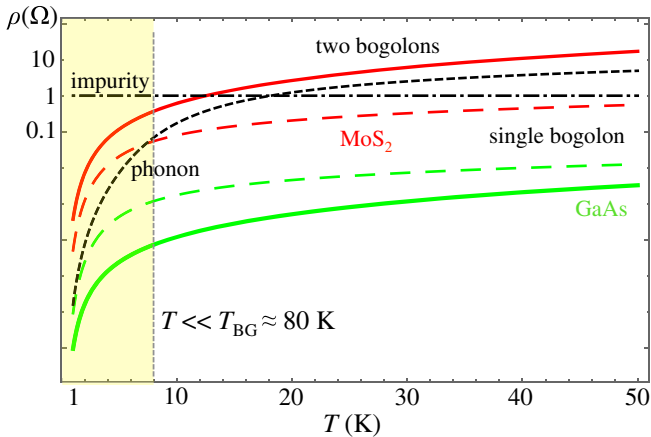


FIG. 3. Resistivity as a function of temperature for MoS₂ (red) and GaAs (green) exciton condensates. Colored solid and dashed curves stand for the two-bogolon and one-bogolon contributions, respectively. Black dash-dotted and dashed curves show the impurity and phonon contributions. We used $n_e = 10^{13} \text{ cm}^{-2}$ and $n_c = 10^9 \text{ cm}^{-2}$.

exciton-polaritons, for which the same treatment is possible (but for different effective mass and the appearance of the Hopfield coefficients), and a degenerate Bose gas (quasi-condensation or superfluidity) was reported there even at room temperature [64]. One can also consider 2DEG in graphene instead of GaAs, where the scattering on impurity is suppressed and mobility is high.

In the conventional approach to hybrid 2DEG BEC systems, the 2b interaction [Eq. (6)] has been disregarded, as it was related to the second-order perturbation theory in fluctuations above the macroscopically occupied ground state. Figure 3 demonstrates that this widespread approximation is not valid in the context of the exciton condensates in MoS₂ material. For GaAs exciton layers, the impurity is dominant for the temperatures 0–3 K at which the condensate can exist. Hence, we will focus on the MoS₂ in what follows.

Figure 4 demonstrates the dependence of resistivity on condensate densities (in the MoS₂-based exciton layer). One sees that the 1b and 2b contributions increase as the condensate density decreases at not-very-high temperatures (blue to green, green to red). This can be understood from Eqs. (11) and (13), giving $\rho^{(1)} \sim \xi_l^2 / (T_{\text{BG}} s^4) \sim n_c^{-1.5}$ and $\rho^{(2)} \sim s^2 / T_{\text{BG}}^3 \sim n_c^{-0.5}$. Note that a similar behavior for the 1b process happens in exciton BEC graphene structures [42]. However, at $T \gg T_{\text{BG}}$, $\rho^{(2)}$ becomes n_c independent, as follows from Eq. (14) and Fig. 4, where red, green, and blue solid curves start to approach each other at higher temperatures. We further note that the BEC-related screening on impurity and phonon processes has no significant effect; therefore, we plot only two curves for them.

We want to emphasize that these observations are valid as long as n_c is macroscopically large. There are two reasons for this limitation. First, in our calculations, we

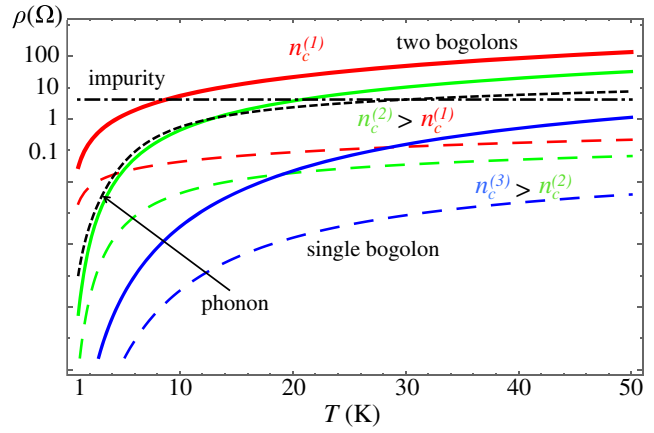


FIG. 4. Temperature dependence of resistivity for various MoS₂ condensate densities: $n_c = 10^8 \text{ cm}^{-2}$ (red), $n_c = 10^{10} \text{ cm}^{-2}$ (green), and $n_c = 10^{11} \text{ cm}^{-2}$ (blue). The corresponding Bloch-Grüneisen temperatures are ~ 17 , 174 and 549 K, respectively. The electron density is fixed: $n_e = 5 \times 10^{12} \text{ cm}^{-2}$.

assume that the bogolon dispersion is linear [49]. This remains valid for $n_c \gtrsim 10^8 \text{ cm}^{-2}$. Second, even if we were to relax this assumption, we note that the replacement of the exciton field operator by $\Phi_{\mathbf{R}} = \sqrt{n_c} + \varphi_{\mathbf{R}}$, where n_c is treated as an ordinary complex number instead of an operator, is a mean field approach, which is an essential ingredient of the Bogoliubov theory. Hence, we cannot expand our conclusions to the $n_c \rightarrow 0$ limit. However, we expect that in this limit the bogolon contribution should vanish and be replaced by the bare exciton contribution, dictated by $u_p = 1$ and $v_p = 0$ in Eqs. (5) and (6).

The dependence of resistivity on the separation between the layers l turns out to be rather strong, as expected, and the dependence on the sample size L (for 2b scattering, where we introduced the infrared cutoff) is weak (see the Supplemental Material [49]). This allows us to optimize the design of the sample by changing l , keeping in mind that L does not (qualitatively) influence the physical phenomena in question.

The bogolon, impurity, and phonon-mediated resistivities all depend on the density of carriers of charge in the 2DEG (see Fig. 5), generally decreasing with the increase of n_e . However, they do so at different rates. For example, at $n_e = 10^{13} \text{ cm}^{-2}$, the impurity is dominant in the temperature interval ~ 0 –20 K, while both the bogolon pair and phonons become dominant (and have comparable contributions) for $T \sim 20$ –50 K. At lower $n_e = 10^{11} \text{ cm}^{-2}$, the bogolon pair starts to give the largest contribution at $T \gtrsim 5$ K, even reaching 2 orders of magnitude greater than the contribution of impurities at 50 K.

The dominance of the 2b channel over the 1b scattering in MoS₂ exciton layer can be understood from the analysis of the matrix elements in the Fermi golden rule. In the 1b case, there appears a small factor $(u_p + v_{-p}) \sim \sqrt{1 + A^2} - A$, where $A = (Ms)/(\hbar\lambda)$ [49]. In other words,

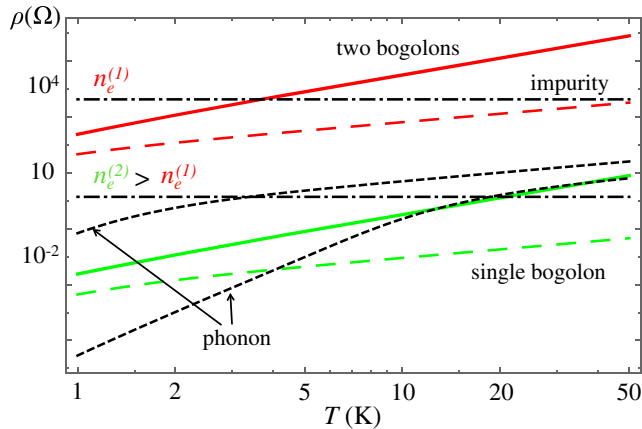


FIG. 5. Temperature dependence of 1b and 2b resistivities at different electron densities: $n_e = 10^{11}$ (red) and $n_e = 10^{13} \text{ cm}^{-2}$ (green). The corresponding Bloch-Grüneisen temperatures are ~ 2 and 25 K , respectively. The density of the MoS_2 condensate is taken to be $n_c = 10^8 \text{ cm}^{-2}$. The dash-dotted and dashed curves show the corresponding impurity and phonon-mediated resistivities.

$(u_{\mathbf{p}} + v_{-\mathbf{p}}) \sim (p\xi)^2 \ll 1$. In particular, in MoS_2 material, this factor is sufficiently small to compensate the large value of $\sqrt{n_c}$. In contrast, there is no such cancellation effect in the 2b terms, where there appears the product $u_{\mathbf{p}}v_{\mathbf{p}} \sim (p\xi)^{-1} \gg 1$ (instead of $u_{\mathbf{p}} + v_{-\mathbf{p}}$). Here we would like to draw a comparison with acoustic phonons, where this cancellation effect does not take place, so that the single-phonon scattering has a larger contribution than the two-phonon scattering. This argument manifests the difference between the bogolon and phonon-assisted scattering, which is due to the difference in the origin of Coulomb interaction between the particles.

In an experiment, it might be difficult to resolve different contributions to the total resistivity, especially at low T . However, using the analytical formula in Eq. (14), we predict that the high-temperature resistivity should behave as $\sim T^2$, if the 2b scattering gives the dominant contribution. This is in contrast with phonons, which give $\sim T$ and impurities with nearly absent T dependence.

What can we say about the electron pairing in such a hybrid 2DEG BEC system below T_c ? For any metal in the normal (not superconducting) state, the strength of electron-phonon interaction is responsible for the resistivity due to the scattering. Obviously, the stronger the interaction strength (which is mostly determined by the matrix element of interaction), the larger the resistivity. In the superconducting phase, the electron pairing is also mediated by the interaction with phonons (or bogolons [5]). Indeed, there enters the same matrix element of the electron-phonon interaction. The bigger it is, the larger the superconducting gap opens, which means a robust superconductivity. The critical temperature is also determined by the strength of the electron-phonon (bogolon)

interaction. It makes us suppose that *bad* conductors in the normal phase are *good* superconductors and suggests an alternative mechanism of high-temperature bogolon-pair-mediated superconductivity.

In conclusion, we have studied the transport of electrons coupled with a two-dimensional Bose-Einstein-condensed dipolar exciton gas via the Coulomb interaction. We calculated the resistivity using and extending the Bloch-Grüneisen approach and provided analytical formulas for the single- and two-bogolon scattering channels, discovering that two-bogolon scattering can be the dominant mechanism in hybrid systems in certain ranges of temperatures. Furthermore, we suggested an alternative way of electron pairing mediated by a pair of bogolons.

We have been supported by the Institute for Basic Science in Korea (Project No. IBS-R024-D1), the Russian Science Foundation (Project No. 17-12-01039), and the Russian Foundation for Basic Research (Project No. 18-29-20033).

- [1] J. D. Sau, R. M. Lutchyn, S. Tewari, and S. Das Sarma, *Phys. Rev. Lett.* **104**, 040502 (2010).
- [2] J. Alicea, *Phys. Rev. B* **81**, 125318 (2010).
- [3] V. Mourik, K. Zuo, S. M. Frolov, S. R. Plissard, E. P. A. M. Bakkers, and L. P. Kouwenhoven, *Science* **336**, 1003 (2012).
- [4] H. J. Suominen, M. Kjaergaard, A. R. Hamilton, J. Shabani, C. J. Palmstrøm, C. M. Marcus, and F. Nichele, *Phys. Rev. Lett.* **119**, 176805 (2017).
- [5] F. P. Laussy, A. V. Kavokin, and I. A. Shelykh, *Phys. Rev. Lett.* **104**, 106402 (2010).
- [6] O. Cotlet, S. Zeytinoğlu, M. Sigrist, E. Demler, and A. İmamoğlu, *Phys. Rev. B* **93**, 054510 (2016).
- [7] P. Skopelitis, E. D. Cherotchenko, A. V. Kavokin, and A. Posazhennikova, *Phys. Rev. Lett.* **120**, 107001 (2018).
- [8] J. Kasprzak, M. Richard, S. Kundermann, A. Baas, P. Jeambrun, J. M. J. Keeling, F. M. Marchetti, M. H. Szymańska, R. André, J. L. Staehli, V. Savona, P. B. Littlewood, B. Deveaud, and L. S. Dang, *Nature (London)* **443**, 409 (2006).
- [9] O. L. Berman and R. Y. Kezerashvili, *Phys. Rev. B* **93**, 245410 (2016).
- [10] V. P. Kochereshko *et al.*, *Sci. Rep.* **6**, 20091 (2016).
- [11] M. V. Boev, V. M. Kovalev, and I. G. Savenko, *Phys. Rev. B* **94**, 241408(R) (2016).
- [12] K. H. A. Villegas, V. M. Kovalev, F. V. Kusmartsev, and I. G. Savenko, *Phys. Rev. B* **98**, 064502 (2018).
- [13] M. Matuszewski, T. Taylor, and A. V. Kavokin, *Phys. Rev. Lett.* **108**, 060401 (2012).
- [14] M. Bibes, J. E. Villegas, and A. Barthélémy, *Adv. Phys.* **60**, 5 (2011).
- [15] S. C. Singhal and K. Kendall, *High Temperature Solid Oxide Fuel Cells: Fundamentals, Design, and Applications* (Oxford Press, Oxford, 2003).
- [16] S. M. Sze and K. K. Ng, *Physics of Semiconductor Device* (John Wiley & Sons, New York, 2007).

- [17] S. Seri and L. Klein, *Phys. Rev. B* **80**, 180410(R) (2009).
- [18] N. Reyren, M. Bibes, E. Lesne, J.-M. George, C. Deranlot, S. Collin, A. Barthélémy, and H. Jaffrèse, *Phys. Rev. Lett.* **108**, 186802 (2012).
- [19] J. Zhou, W.-Y. Shan, and D. Xiao, *Phys. Rev. B* **91**, 241302 (R) (2015).
- [20] A. Ohtomo and H. Y. Hwang, *Nature (London)* **427**, 423 (2004).
- [21] G. Khalsa and A. H. MacDonald, *Phys. Rev. B* **86**, 125121 (2012).
- [22] N. Ganguli and P. J. Kelly, *Phys. Rev. Lett.* **113**, 127201 (2014).
- [23] H. Y. Hwang, Y. Iwasa, M. Kawasaki, B. Keimer, N. Nagaosa, and Y. Tokura, *Nat. Mater.* **11**, 103 (2012).
- [24] J. T. Haraldsen, P. Wölfle, and A. V. Balatsky, *Phys. Rev. B* **85**, 134501 (2012).
- [25] P. Kumar, P. Pal, A. K. Shukla, J. J. Pulikkotil, and A. Dogra, *Phys. Rev. B* **91**, 115127 (2015).
- [26] D. Jena and A. Konar, *Phys. Rev. Lett.* **98**, 136805 (2007).
- [27] T. M. Gibbons and S. K. Estreicher, *Phys. Rev. Lett.* **102**, 255502 (2009).
- [28] L. Shi and L.-W. Wang, *Phys. Rev. Lett.* **109**, 245501 (2012).
- [29] J. C. Bourgoin and M. Zazoui, *Phys. Rev. B* **45**, 11324 (1992).
- [30] D. G. Eshchenko, V. G. Storchak, J. H. Brewer, and R. L. Lichti, *Phys. Rev. Lett.* **89**, 226601 (2002).
- [31] A. Palma, J. A. Jiménez-Tejada, A. Godoy, J. A. López-Villanueva, and J. E. Carceller, *Phys. Rev. B* **51**, 14147 (1995).
- [32] M. V. Boev, V. M. Kovalev, and I. G. Savenko, *Phys. Rev. B* **97**, 165305 (2018).
- [33] D. Di Sante and S. Ciuchi, *Phys. Rev. B* **90**, 075111 (2014).
- [34] T. Kawamura and S. Das Sarma, *Phys. Rev. B* **45**, 3612 (1992).
- [35] H. Gummel and M. Lax, *Phys. Rev.* **97**, 1469 (1955).
- [36] M. Lax, *Phys. Rev.* **119**, 1502 (1960).
- [37] V. N. Abakumov and I. N. Yassievich, *Zh. Eksp. Teor. Fiz.* **71**, 657 (1976)[*Sov. Phys. JETP* **44**, 345 (1976)].
- [38] E. V. Kirichenko, V. A. Stephanovich, and V. K. Dugaev, *Phys. Rev. B* **95**, 085305 (2017).
- [39] V. M. Kovalev and A. V. Chaplik, *JETP Lett.* **94**, 560 (2011).
- [40] V. M. Kovalev and A. V. Chaplik, *JETP Lett.* **98**, 331 (2013).
- [41] E. G. Batyev, V. M. Kovalev, and A. V. Chaplik, *JETP Lett.* **99**, 540 (2014).
- [42] M. Sun, K. H. A. Villegas, V. M. Kovalev, and I. G. Savenko, *Phys. Rev. B* **99**, 115408 (2019).
- [43] L. Butov, *Superlattices Microstruct.* **108**, 2 (2017).
- [44] L. B. M. M. Fogler and K. Novoselov, *Nat. Commun.* **5**, 4555 (2014).
- [45] L. Butov, *Solid State Commun.* **127**, 89 (2003).
- [46] S. Giorgini, *Phys. Rev. A* **57**, 2949 (1998).
- [47] J. Ziman, *Electrons and Phonons: The Theory of Transport Phenomena in Solids* (Oxford University Press, Oxford, 2001).
- [48] R. O. Zaitsev, *Introduction to Modern Kinetic Theory* (URSS editorial, Moscow, 2014).
- [49] See Supplemental Material at <http://link.aps.org/supplemental/10.1103/PhysRevLett.123.095301> for the detailed derivations.
- [50] V. Bagnato and D. Kleppner, *Phys. Rev. A* **44**, 7439 (1991).
- [51] P. C. Hohenberg, *Phys. Rev.* **158**, 383 (1967).
- [52] T. Kawamura and S. Das Sarma, *Phys. Rev. B* **45**, 3612 (1992).
- [53] S. J. MacLeod, K. Chan, T. P. Martin, A. R. Hamilton, A. See, A. P. Micolich, M. Aagesen, and P. E. Lindelof, *Phys. Rev. B* **80**, 035310 (2009).
- [54] H. Min, E. H. Hwang, and S. Das Sarma, *Phys. Rev. B* **86**, 085307 (2012).
- [55] E. E. Mendez, P. J. Price, and M. Heiblum, *Appl. Phys. Lett.* **45**, 294 (1984).
- [56] K. Hirakawa and H. Sakaki, *Phys. Rev. B* **33**, 8291 (1986).
- [57] A. Gold, *Phys. Rev. B* **41**, 8537 (1990).
- [58] The values of parameters were taken from Refs. [59–61]. Dielectric constants: $\epsilon_{\text{GaAs}} = 12.5\epsilon_0$, $\epsilon_{\text{MoS}_2} = 4.89\epsilon_0$. Effective electron masses (m_0 is the bare electron mass): $m_{\text{GaAs}} = 0.067m_0$, $m_{\text{MoS}_2} = 0.47m_0$. Exciton masses: $M_{\text{GaAs}} = 0.517m_0$, $M_{\text{MoS}_2} = 0.499m_0$. Exciton sizes: $d_{\text{GaAs}} = 10.0 \text{ nm}$, $d_{\text{MoS}_2} = 3.5 \text{ nm}$. Deformation potential: $D_{\text{GaAs}} = 12 \text{ eV}$.
- [59] K. Kaasbjerg, K. S. Thygesen, and A.-P. Jauho, *Phys. Rev. B* **87**, 235312 (2013).
- [60] P. K. Basu and B. R. Nag, *Phys. Rev. B* **22**, 4849 (1980).
- [61] E. G. R. A. Mair, R. Preposty, and T. Maruyama, *Phys. Lett. A* **239**, 277 (1998).
- [62] E. H. Hwang and S. Das Sarma, *Phys. Rev. B* **77**, 235437 (2008).
- [63] M. J. Manfra, *Annu. Rev. Condens. Matter Phys.* **5**, 347 (2014).
- [64] G. Lerario, A. Fieramosca, F. Barachati, D. Ballarini, K. S. Daskalakis, L. Dominici, M. De Giorgi, S. A. Maier, G. Gigli, S. Kéna-Cohen, and D. Sanvitto, *Nat. Phys.* **13**, 837 (2017).